



Adipose tissue (P)RR regulates insulin sensitivity, fat mass and body weight

Zulaykho Shamansurova^{1,2,5,7}, Paul Tan^{1,3,5,7}, Basma Ahmed^{1,2}, Emilie Pepin^{1,5}, Ondrej Seda^{1,6}, Julie L. Lavoie^{1,4,5,*}

ABSTRACT

Objective: We previously demonstrated that the handle-region peptide, a prorenin/renin receptor [(P)RR] blocker, reduces body weight and fat mass and may improve insulin sensitivity in high-fat fed mice. We hypothesized that knocking out the adipose tissue (P)RR gene would prevent weight gain and insulin resistance.

Methods: An adipose tissue-specific (P)RR knockout (KO) mouse was created by Cre-loxP technology using AP2-Cre recombinase mice. Because the (P)RR gene is located on the X chromosome, hemizygous males were complete KO and had a more pronounced phenotype on a normal diet (ND) diet compared to heterozygous KO females. Therefore, we challenged the female mice with a high-fat diet (HFD) to uncover certain phenotypes. Mice were maintained on either diet for 9 weeks.

Results: KO mice had lower body weights compared to wild-types (WT). Only hemizygous male KO mice presented with lower total fat mass, higher total lean mass as well as smaller adipocytes compared to WT mice. Although food intake was similar between genotypes, locomotor activity during the active period was increased in both male and female KO mice. Interestingly, only male KO mice had increased O₂ consumption and CO₂ production during the entire 24-hour period, suggesting an increased basal metabolic rate. Although glycemia during a glucose tolerance test was similar, KO males as well as HFD-fed females had lower plasma insulin and C-peptide levels compared to WT mice, suggesting improved insulin sensitivity. Remarkably, all KO animals exhibited higher circulating adiponectin levels, suggesting that this phenotype can occur even in the absence of a significant reduction in adipose tissue weight, as observed in females and, thus, may be a specific effect related to the (P)RR.

Conclusions: (P)RR may be an important therapeutic target for the treatment of obesity and its associated complications such as type 2 diabetes.

© 2016 The Author(s). Published by Elsevier GmbH. This is an open access article under the CC BY-NC-ND license (<http://creativecommons.org/licenses/by-nc-nd/4.0/>).

Keywords (Pro)renin receptor; Renin-angiotensin system; Adipose tissue knock-out mice; Obesity; Adipose tissue; Insulin resistance

1. INTRODUCTION

Obesity and type 2 diabetes constitute worldwide pandemics [1,2]. Finding effective ways to prevent and treat these diseases is of major clinical and economic importance. The study of patients suffering from obesity and obese rodent models has shed light on the importance of the renin-angiotensin system (RAS) in the development of obesity [3,4]. In particular, adipose tissue RAS has been found to be increased in this condition, along with adipose tissue hypoxia and inflammation [5]. Those changes lead to compromised adipocyte function characterized by abnormal adipokine secretion and glucose and lipid metabolism, which together cause insulin resistance and increase the risk of developing type 2 diabetes [5]. Indeed, overexpression of

angiotensinogen (Agt) in rodents, specifically in adipose tissue, causes obesity and insulin resistance, while systemic suppression of RAS genes protects from high-fat diet (HFD) induces obesity and improves insulin sensitivity [6]. In addition, clinical studies have shown that RAS inhibitors routinely used as anti-hypertensive treatments also improve insulin sensitivity and glucose homeostasis and prevent cardiovascular complications in diabetic patients [5].

The prorenin/renin receptor [(P)RR] has been shown to be a component of the RAS where its main role is to produce a non-proteolytic activation of prorenin and increase the catalytic activity of renin to cleave Agt into angiotensin I (Ang I) [7]. Ang I is then converted by the Ang converting enzyme to Ang II, the main physiologically active peptide of this system [8]. Ang II, via activation of many pathways, promotes cell

¹Centre de Recherche du Centre Hospitalier de l'Université de Montréal (CRCHUM), Université de Montréal, Québec, Canada ²Department of Physiology, Université de Montréal, Québec, Canada ³Department of Biochemistry and Molecular Medicine, Université de Montréal, Québec, Canada ⁴Department of Kinesiology, Université de Montréal, Québec, Canada ⁵Montreal Diabetes Research Center, Québec, Canada ⁶First Faculty of Medicine, Charles University in Prague, Prague, Czech Republic

⁷ These authors contributed equally to this work.

*Corresponding author. Centre de Recherche du CHUM, 900 St-Denis Street, Tour Viger, R08.452, Montréal, Québec, H2X 0A9, Canada. Fax: +1 (514) 412 7655. E-mail: julie.lavoie.3@umontreal.ca (J.L. Lavoie).

Abbreviations: ANG, Angiotensin; BAT, brown adipose tissue; BB, beam break; HACT, horizontal activity; HFD, high-fat diet; HRP, handle-region peptide; KO, knock-out; ND, normal diet; OGTT, oral glucose tolerance test; PGF, perigonadal fat; PPAR- γ , peroxisome proliferator-activated receptor- γ ; PRA, plasma renin activity; PRF, perirenal fat; (P)RR, prorenin/renin receptor; RAS, renin-angiotensin system; SE, standard error; SFC, abdominal subcutaneous fat; SM, skeletal muscle; SMG, submandibular gland; TG, triglycerides; V-ATPase, vacuolar proton pump H⁺-ATPase; VCO₂, carbon dioxide production; VO₂, oxygen consumption; WT, wild-type

Received August 3, 2016 • Revision received August 12, 2016 • Accepted August 16, 2016 • Available online 23 August 2016

<http://dx.doi.org/10.1016/j.molmet.2016.08.009>

proliferation, fibrosis, and apoptosis, which could lead to obesity-related complications, such as type 2 diabetes [9,10]. Simultaneously, binding of prorenin/renin to the (P)RR activates Ang II-independent pathways, including mitogen-activated protein kinases and tumor growth factor beta, which may also contribute to end-organ damage [11]. Unfortunately, the RAS inhibitors currently used clinically all cause a compensatory increase in plasma renin concentrations and, as a result, may increase (P)RR Ang II-independent pathways as these drugs do not prevent renin from binding to the (P)RR [12,13].

Independently of prorenin/renin binding, the (P)RR (also known as ATP6AP2) acts as an adapter to the cell membrane vacuolar proton pump H⁺-ATPase (V-ATPase), and consequently activates Wnt signaling [11]. Given that this signaling cascade is implicated in embryogenesis, whole-body suppression of the (P)RR is lethal [14,15]. Moreover, mice with specific (P)RR gene suppression in the heart or kidneys die at 2–4 weeks of age [16,17].

Our previous results showed that obese mice and insulin resistant obese women have increased adipose tissue (P)RR expression [18]. Furthermore, we demonstrated that systemic treatment of HFD-fed mice with the handle region peptide (HRP), a (P)RR blocker, reduces body weight gain and visceral fat masses and may improve insulin sensitivity [18], similarly to what is observed in models of RAS gene suppression [6]. The aim of the present study was to better understand the role of adipose tissue (P)RR in the metabolic effects induced by HRP treatment in the context of obesity using adipose tissue specific (P)RR KO mice.

2. MATERIALS AND METHODS

2.1. Generation of adipose-tissue specific (P)RR KO mice

To produce mice with the (P)RR gene deleted specifically in adipose tissue, mice expressing the Cre-recombinase specifically in adipose tissue under the control of the AP2 promoter (AP2-Cre^{Salk} mice; [19,20]; #005069, Jackson Lab) were bred with mice with loxP sites flanking the (P)RR exon 2 between locus 2271–2276 ((P)RR-Loxp mice; a generous gift from Merck Frosst Canada) (Supplemental Figure 1). As the (P)RR gene is present on the X chromosome [11], male mice were homozygous KOs while female mice were heterozygous KOs.

2.2. Animals

Mice were placed in individual cages at 10 weeks of age and were maintained on a normal diet (ND; #2918, Teklad Global, Harlan Laboratories, Madison, WI, USA) and 12-h light/dark cycle. Starting at 12 weeks of age, mice were maintained on the ND or switched to a HFD (Bio-Serv F3282, Frenchtown, NJ, USA) for 9 weeks. Mice had access to water and food *ad libitum*. Body weight and food intake were measured weekly from 12 to 17 weeks of age. Care of the mice used in these experiments complied with standards for the care and use of experimental animals set by the Canadian Council for the Protection of Animals, and all procedures were approved by the university's Animal Care and Use Committee at the CHUM Research Center.

2.3. Mouse genotyping

Mouse genotypes were determined using genomic DNA from mouse tail snips extracted by hot-shot NaOH-EDTA protocol [21,22]. PCR were then performed using specific primers (IDT IL, USA) detailed in Supplementary Table 1. Each reaction contained 1 μ l 10 \times buffer, 0.2 μ l 10 mM dNTP, 0.1 μ l of each primer, 6.4 μ l of water, 0.5 μ l Taq polymerase (Feldan, Bio-Basic, Markham, ON, Canada), and 2 μ l of

genomic DNA, as described previously [23]. PCR products were subsequently analyzed on 1% or 3% agarose gels containing SYBR Green (Invitrogen by Life Technologies, Carlsbad, CA, USA).

2.4. Adipose tissue specificity of the KO model

The tissue specificity of our KO model was confirmed by real-time PCR using the primers listed in Supplementary Table 1. For this purpose, 12 week-old male mice were sacrificed, and different white adipose tissue depots (abdominal subcutaneous fat (SCF) and visceral fat (perigonadal fat (PGF) and perirenal fat (PRF)) were collected, weighed, flash frozen, and analyzed by real-time PCR. (P)RR gene expression was assessed in the different white adipose tissue depots as well as in other tissues such as, brown adipose tissue (BAT), heart, spleen, gonads, kidneys, submandibular gland, pancreas, liver, brain, adrenal glands, skeletal muscle, lung, diaphragm, and aorta.

2.5. Reverse transcription and qPCR gene expression

Tissue RNA was extracted using Trizol reagent (Invitrogen, Burlington, ON, Canada) according to the manufacturer's protocol. To remove genomic DNA, RNA samples were incubated with deoxyribonuclease I (2U per μ g RNA) for 30 min at 37 °C. Single-stranded cDNA was synthesized by reverse-transcriptase reaction using SuperScript II Reverse Transcriptase (FisherScientific, Ottawa, ON, Canada). The RT-PCR final volume was 10 μ l and contained 0.3 μ mol/l of the specific forward (F) and reverse (R) primers [24] listed in Supplementary Table 1, as well as 2.5 μ l of single-stranded cDNA template. The amplification was done using Faststart SYBR Green Master fluorescent dye (04 673 492 001; ROCHE, Mississauga, ON, Canada) using the Rotor Gene RG-3000 (Corbett Research).

2.6. Survival rate and fetal weight

We compared fetal weights in litters obtained from 8 pregnant mice (3–11 pups/litter), produced using the breeding protocol mentioned above, on the 17th day of gestation.

2.7. Body composition

Fat and lean body masses were analyzed using an Echo-MRI-100TM apparatus (Echo Medical Systems, Houston Scientific, Houston, TX, USA) both at the beginning and at the end of the protocol (at 12 and 20 weeks of age, respectively).

2.8. Mouse locomotor activity and indirect calorimetry

Mouse locomotor activity and metabolic parameters were studied in metabolic cages at 18 weeks of age (AccuScan Instruments, Columbus, OH, USA), and data were analyzed according to Ferrannini et al., 1988 [25]. After 3 days of acclimation, locomotor activity was evaluated by infrared beam interruptions by mouse movement in the horizontal and vertical axis, while metabolic parameters were assessed (oxygen consumption (VO₂) and carbon dioxide production (vCO₂)) for 24 h. Data were summarized for both the light and dark cycles [26].

2.9. Oral glucose tolerance test (OGTT)

At 20 weeks of age, an OGTT was performed after overnight (16–17 h) fasting. Dextrose (Hospira, Inc. Lake Forest, IL, USA) was administered orally by gavage at a dose of 2 g/kg for ND-fed mice or 5 g/kg for HFD-fed mice [27–29]. Blood was collected from the tail vein at baseline (T0) and 15, 30, 45, 60, and 120 min after gavage using a glucometer (Accu-Chek Performa, Roche, Indianapolis, IN, USA). Plasma was also collected at baseline (T0) and 30 min after gavage using glass capillaries (Precision, MO, USA), then transferred into BD vacutainer tube and separated by centrifugation (Becton, Dickinson, Mississauga, ON,

Canada) for measurement of insulin and C-peptide levels, as described below.

2.10. Mouse necropsy and organ collection

At the end of the protocol (21 weeks of age), mice were anesthetized, blood was collected by intrathoracic cardiac puncture using the anti-coagulant EDTA. Plasma was then isolated by centrifugation and stored at -80°C . White adipose tissue (SCF, PGF and PRF) and other organs (BAT, liver, pancreas, and skeletal muscle) were collected and weighed. All samples were flash frozen and kept at -80°C until further analysis. Tibia was also collected and its length was measured using a caliper.

2.11. Circulating parameters

Plasma triglycerides (TG) and glycerol were measured using a Serum Triglyceride Determination Kit (Sigma, Oakville, Canada) following the manufacturer's protocol. Plasma insulin, C-peptide, adiponectin and leptin levels were measured using bead-based AlphaLISA immunoassay kits (Perkin Elmer, Waltham, MA) according to the manufacturer's instructions. Plasma renin activity was calculated by measuring Angiotensin I production by immunoassay kit (Diagnostic Biochem Canada, Dorchester, ON, Canada).

2.12. Tissue TG and glycerol content

Frozen liver samples were powdered, and 40–60 mg were used for the assay. TGs were extracted by homogenization and incubation with 0.5 M KOH in ethanol for 20 min at 70°C . Supernatant was separated with 0.15 M MgSO_4 solution by centrifugation at 5000 rpm for 5 min. TGs were measured as described above for plasma TG. Glycerol and TG levels in skeletal muscle (soleus and plantaris combined) were measured as for the liver, with prior extraction in 20 mMol TRIS-HCL buffer containing protease inhibitors [30,31].

2.13. Total pancreatic insulin content

Pancreatic insulin content was measured by extraction of frozen whole organ powder in acidic ethanol as described [32]. Pancreatic acid-ethanol extracts were centrifuged at 3000 g for 15 min at 4°C and supernatants were collected. After an additional centrifugation, pancreas insulin was measured as described above for insulin in plasma. Results were normalized by tissue weight.

2.14. Histology and immunohistochemistry

Adipose tissue was fixed in 10% formalin, embedded in paraffin, and sectioned using a microtome. Hematoxylin-Eosin stained slides were used for light microscopy. Embedding, sectioning, and staining were performed by the histology platform of the Research Institute in Immunology and Cancerology at the Université de Montréal. Adipocyte size was calculated in defined $2.33 \times 1.73 \mu\text{m}$ square in 3 randomly selected digital photographic images taken for each fat pads per mouse under the $100\times$ magnification using an Olympus 600 (MA, USA) light microscope and "Q-capture" software. Data were analyzed using Image-J software [33,34]. A subset of samples was deparaffinized, using 3 consecutive incubations in xylene for 5 min, and then rehydrated with 95% ethanol for 5 min. Slides were then heated in a microwave for 10 min in 10 mmol/L sodium citrate (pH 6.0) for antigen retrieval, incubated with 3% hydrogen peroxide for 20 min, blocked with 5% BSA (Roche Diagnostics, Germany) in 1.0 ml PBS for 30 min at room temperature (RT), and then incubated with goat anti-(P)RR antibody (#SAB2500134, Sigma Aldrich, Missouri, USA) at a 1:25 dilution in 1% BSA for 2 h at room temperature (RT). Finally, we used Alexa Fluorescent 555-Donkey anti-goat IgG (#AB150134, Life

Technology, NY, USA) at a 1:200 dilution in 1% BSA for 1 h at RT. Signals were observed using an immunoluminescence microscope (Nikon eclipse TE2000-5) [35] and were digitalized using a QICAM imaging system.

2.15. Statistical analysis

All data are presented as mean \pm standard error (SE). Differences between the groups for single measurements were evaluated by *t*-test. Two-way repeated measure ANOVA was used for analysis when comparing groups and different time points. When a significant interaction was detected, a Tukey post-hoc analysis was performed. Data were considered to be statistically significant when $p < 0.05$.

3. RESULTS

3.1. Validation of AP2-Cre/(P)RR flox KO specificity

(P)RR gene deletion was first analyzed by real-time PCR in complete KO and WT ND-fed male mice in the various adipose depots and additional tissues (Supplemental Figure 2a and b). We found that the (P)RR gene expression was significantly decreased in KO mice compared to WT mice in all white adipose tissue: PGF (37%), PRF (49%) and SCF (51%) (Supplemental Figure 2a). Conversely, no differences were observed in BAT or in any other tissues studied (Supplemental Figure 2a and b). These results confirmed the tissue specificity of our KO model. The adipocyte specificity was then validated using immunofluorescent staining of histological sections. Indeed, both male and female KO mice had reduced fluorescent signals (close to no signal in males) in adipocyte membranes of all white adipose tissue analyzed compared to WT (Supplementary Figure 3).

3.2. Male KO mouse survival rate is lower compared to females during development

The litter size was assessed in 8 ND-fed dams at day 17 of gestation. We found significantly more female than male pups ($66.2 \pm 3.7\%$ vs $33.8 \pm 3.7\%$), suggesting that complete deletion of the (P)RR gene in adipose tissue can induce some lethality during embryogenesis. However, despite the reduced number of male pups per litter, male fetal body weights were, in accordance with the literature, in general 2–7% heavier than female pups without any effect of genotype (Supplementary Table 2) [36].

3.3. Adult KO mice weigh significantly less than WT mice

Despite a similar food intake (Supplementary Table 3), both male and female adult KO mice weighed significantly less than their WT littermates (Figure 1A and B). Indeed, body weight was 23% lower in males on ND and 10% lower in females on both ND and HDF diet at 17 weeks of age (Figure 1B and C). No other visible physical differences could be observed between the KO and WT groups.

3.4. Adult KO male mice are smaller than WT mice

We next investigated whether the (P)RR gene deletion might impact their growth at 21 weeks of age. First we compared mouse size and found that the tibia length of male KOs was 3% shorter than those of WT littermates (Supplementary Table 5). Next, we compared different organ weights and found that male KO mice had significantly lower liver weight expressed as a ratio to tibia length (13%) compared to WT, while heart weight was not different (Supplementary Table 5). Conversely, no differences in tibia length and organ weight could be observed in female mice on either ND or HFD (Supplementary Table 5).

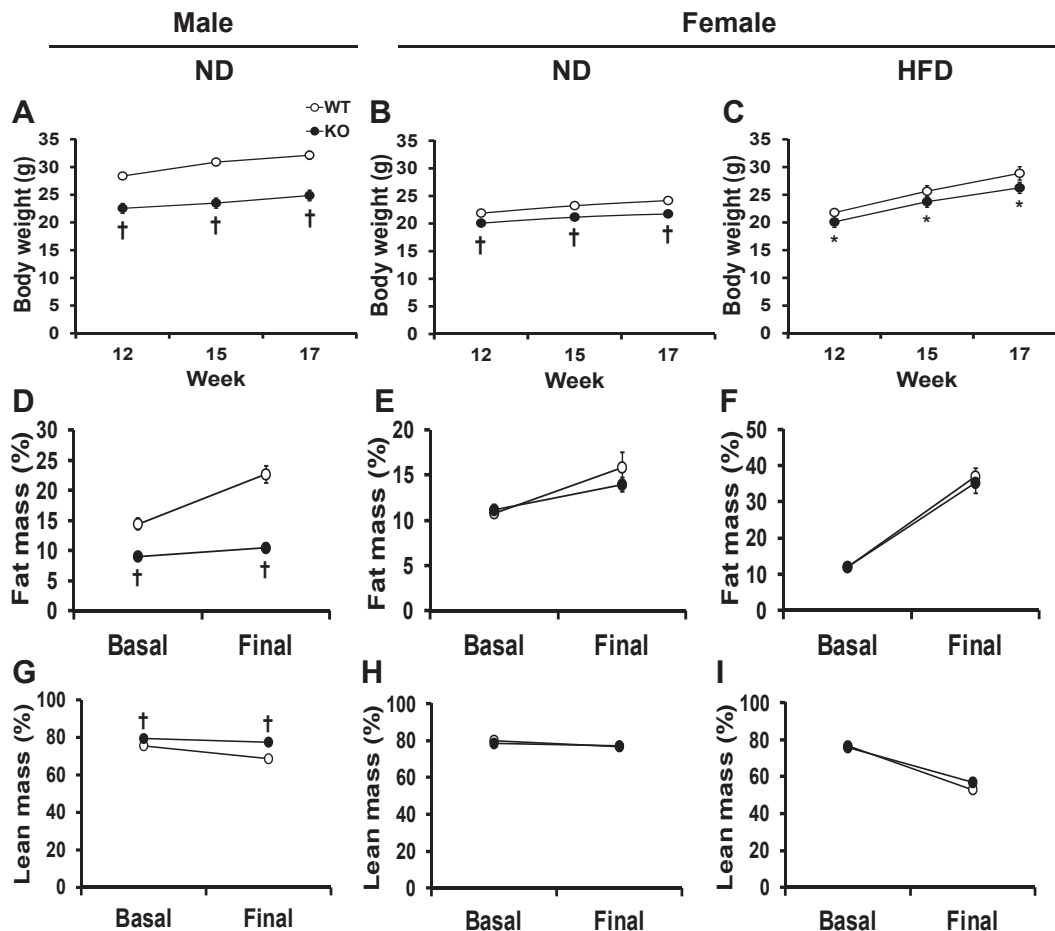


Figure 1: Adipose tissue (PPAR) gene deletion decreases body weight and alters body composition in male mice. Body weight in male mice on ND (A) and female mice on ND (B) and HFD (C) at the beginning (12 weeks), middle (15 weeks) and end (17 weeks) of the diet period. Fat mass and lean mass in male mice on ND (D, G) and in female mice on ND (E and H) and HFD (F and I) at 12 (basal) and 20 (final) weeks of age. Data are presented as mean \pm SE with $n = 6-21$. * $p < 0.05$ and † $p < 0.01$ compared to WT. HFD, high-fat diet; KO, knock-out; ND, normal diet; WT, wild-type.

3.5. Leaner body composition of adult male KO mice

ND-fed male KO mice were found to have significantly lower fat mass normalized to body weight at the beginning (37%; 12 weeks of age) and at the end (54%; 21 weeks of age) of the experiment compared to WT littermates as assessed by EchoMRI (Figure 1D). We also found that lean body mass in ND-fed male KO mice was increased by 5% and 11% at the beginning and end of experiment respectively (Figure 1G). Conversely, no differences in total fat and lean body masses were observed in female mice, either on ND or HFD (Figure 1E, F, H, I).

3.6. Adult KO mice have lighter fat pad masses than WT mice

All fat pad masses were found to be significantly lower (32–53%) in male KO mice compared to WT mice fed ND at 21 weeks of age (Figure 2A). ND-fed female KO mice presented with a significant decrease in SCF (32%) and BAT (21%) weight, whereas PRF tended to be smaller ($p = 0.073$) but without reaching significance while PGF was unchanged (Figure 2A). HFD-fed KO female mice showed no significant decrease in any of the fat pad masses compared to WT (Figure 2A).

3.7. Adipocytes are smaller in adult male KO mice compared to WT

Interestingly, adipose tissue histology demonstrated that adipocytes from visceral fat pads of male KO were significantly smaller in size (40–47%) compared to those from male WT while only a trend was

observed in adipocytes from SCF fat pads ($p = 0.097$) (Figure 2B and C). In contrast, no significant differences in adipocyte size were observed in all fat pads from female KO mice compared to WT fed either diet (Supplementary Table 4). As expected, female WT and KO mice fed a HFD had larger adipocytes compared to ND (Supplementary Table 4).

3.8. KO mice display greater locomotor activity and metabolic rate

Both male and female KO mice fed a ND were significantly more active during their active period (dark cycle), males by 37% and females by 24%, compared to WT mice as a result of increased horizontal activity (Figure 3A and D), while there was no change in vertical activity (Supplementary Table 6). In contrast, we observed no changes in physical activity during their inactive period (light cycle) (Figure 3A,D). In addition, the changes in physical activity observed in male KOs were associated with a significant increase in oxygen consumption (25 and 27%) and in carbon dioxide production (22 and 26%) during the both the dark and light cycles (Figure 3B and C). Conversely, these parameters were unchanged in female mice (Figure 3E and F).

3.9. “Beiging” of adipose tissue may occur in KO mice

“Beiging” is the presence of brown-like adipocytes within white adipose tissue; these brown-like adipocytes are characterized by increased mitochondrial density and small lipid droplets [37]. In male

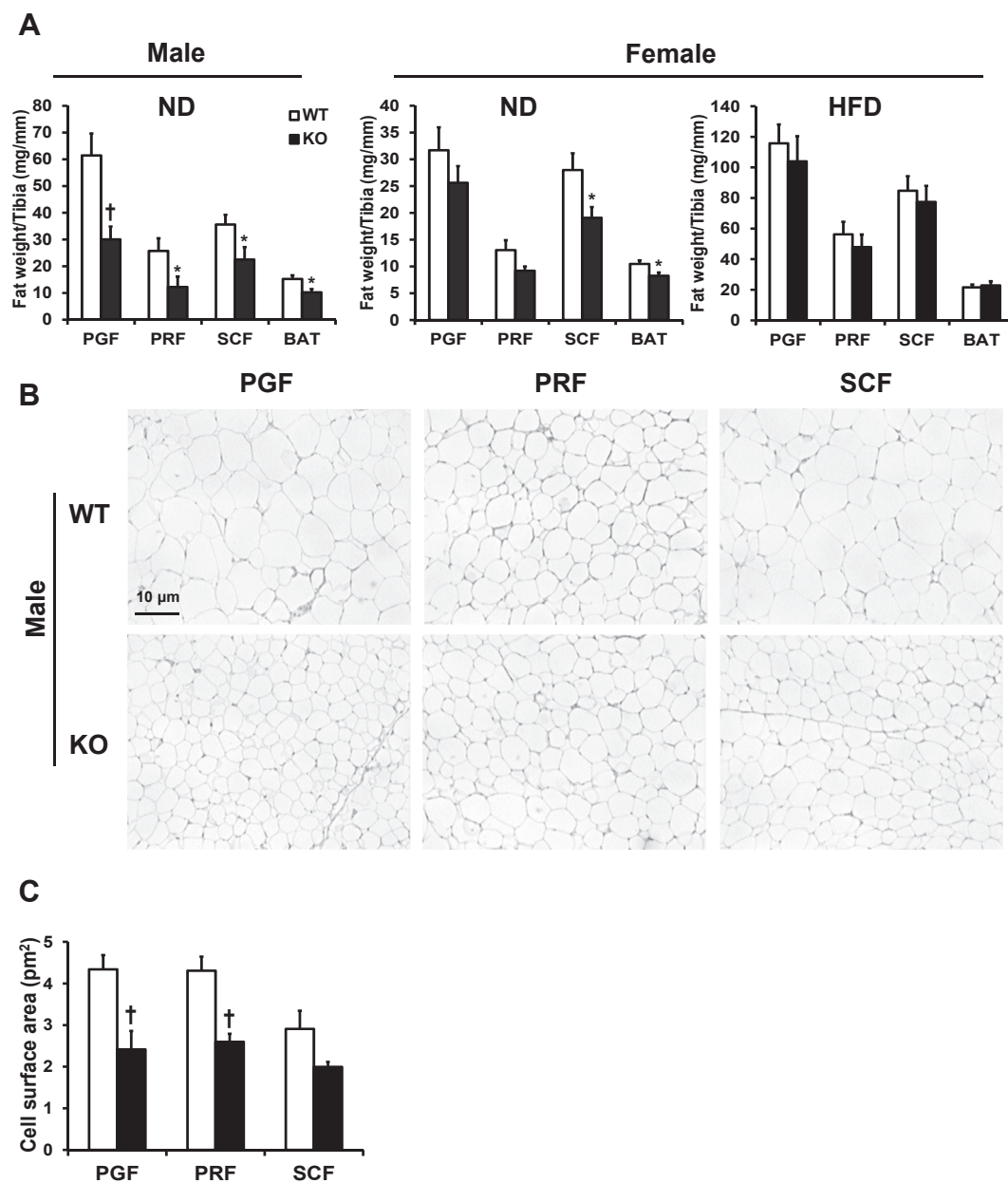


Figure 2: Adipose tissue (P)RR gene deletion decreases fat pad weight in male and female mice on ND and visceral adipocyte size in male mice. Weight of different fat pads in male and female mice fed ND and female mice fed HFD (A). Representative histological sections of visceral and subcutaneous fat pads stained with Hematoxylin-Eosin (scale bar = 10 μ m, magnification = $\times 100$) (B). Quantification of mean adipocyte size from histological sections (C). Data are presented as mean \pm SE with $n = 7-16$. * $p < 0.05$ and † $p < 0.01$ compared to WT. BAT, brown adipose tissue; HFD, high-fat diet; KO, knock-out; ND, normal diet; PGF, perigonadal fat; PRF, perirenal fat; SCF, abdominal subcutaneous fat; WT, wild-type.

KO mice compared to WT littermates, the mRNA expression of *Prdm16*, a marker of “beiging”, was increased by 151% in PRF and decreased by 70% in SCF while it was unchanged in PGF (Figure 4A). *Prdm16* mRNA expression was similar in all fat pads in female mice fed either ND or HFD (Figure 4B).

3.10. KO mice have improved insulin sensitivity compared to WT
 Since (P)RR KO mice are leaner, we hypothesized that they might have improved glucose tolerance and insulin sensitivity. We therefore performed an OGTT, and surprisingly, KO mice had similar glucose tolerance in response to an oral bolus of glucose (Figure 5A–C).

However, male KO mice had markedly lower plasma insulin and C-peptide levels compared to their WT littermates, both at baseline and 30 min after gavage (40–45% and 29–51%, respectively) (Figure 5D and G), indicative of improved insulin sensitivity. Similar observations could be made in HFD-fed female KO mice (Figure 5C,F and I). However, no changes in glucose tolerance, plasma insulin or C-peptide levels could be observed in ND-fed female KO mice (Figure 5B, E, H). Given that the insulin/C-peptide ratios were comparable in all groups (Supplementary Table 7), this strongly suggests that (P)RR deletion in adipose tissue does not affect pancreatic insulin secretion. This is further supported by the fact that total pancreas insulin content was

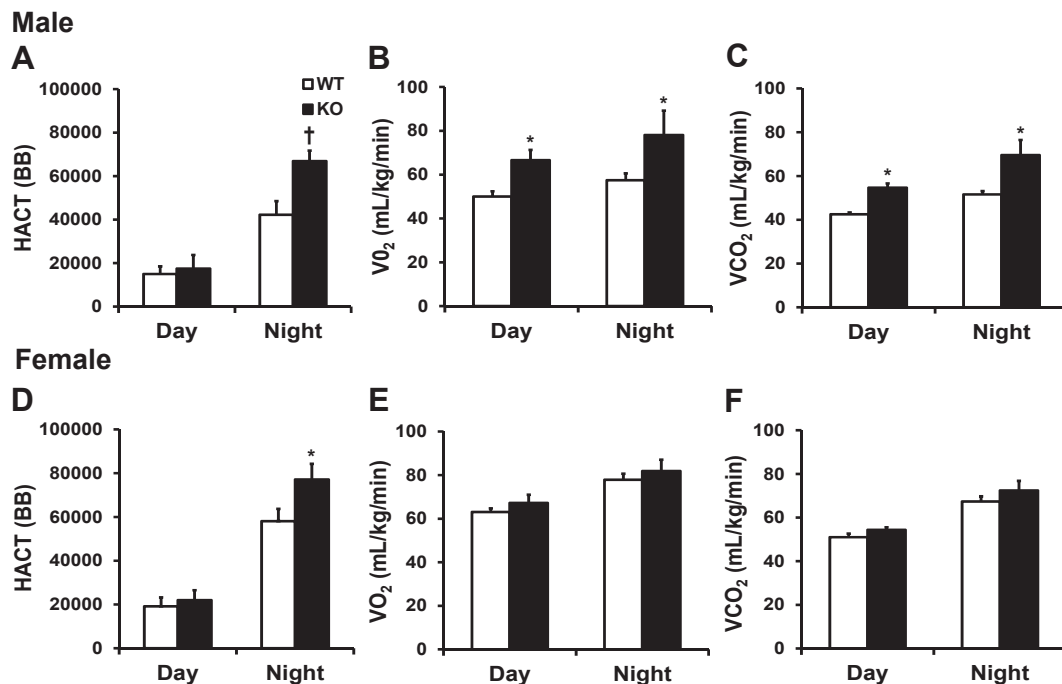


Figure 3: Adipose tissue (P)RR gene deletion increases energy expenditure in male mice. Locomotor activity and metabolic rate (depicted as O₂ consumption and CO₂ production) in male (A, B and C) and female (D, E, and F) mice in light (inactive) and dark (active) cycles. Data are presented as mean \pm SE with $n = 6-11$ per group. * $p < 0.05$ and † $p < 0.01$ compared to WT. BB, beam break; HACT, horizontal activity; VCO₂, carbon dioxide production; VO₂, oxygen consumption; KO, knock-out; WT, wild-type.

similar between KO and WT mice fed either diets (Supplementary Table 8).

3.11. KO mice have different circulating adipokine levels compared to WT

As expected given their important decrease in total fat masses (Figure 1D), leptin levels were significantly lower (3-fold) in male KO mice compared to WT males (Table 1). While no differences could be observed between female KO and WT mice fed either ND or HFD, plasma leptin levels were increased by HFD as expected. Interestingly, we found that circulating adiponectin levels were significantly 1.5-fold higher in male KO mice and 1.4-fold higher in ND and HFD-fed female KO mice compared to their WT littermates (Table 1), which correlates with the improved insulin sensitivity observed during the OGTT.

3.12. Adipose tissue specific (P)RR deletion does not affect circulating lipid levels

Since KO mice presented with lower total fat mass compared to WT mice, we evaluated whether this translated to altered plasma TG levels. However, plasma TG levels were similar in all KO and WT mice (Table 1).

3.13. KO mice have decreased TG content only in skeletal muscles

After adipose tissue, liver and skeletal muscles are two major lipid storage sites [38]. Thus, we verified if (P)RR deletion led to an aberrant storage of lipids in these tissues given their reduced adipose tissue weights. We found that liver TG content was similar between KO and WT mice in both males and females (Supplementary Table 8). In contrast, KO male mice were found to have lower skeletal muscle glycerol (25%) and TG content (61%), compared to WT males fed a ND while no differences could be observed in females fed either diets (Supplementary Table 8).

3.14. Adipose tissue specific (P)RR deletion does not affect plasma renin activity

We found no differences in plasma renin activity between WT and KO mice (Table 1), demonstrating that the (P)RR KO in adipose tissue does not affect circulating RAS activity and as such, systemic RAS modulation did not contribute to the phenotypes observed in KO mice.

4. DISCUSSION

To study the role of adipose tissue (P)RR gene deletion on energy balance, we generated adipose tissue specific KO animals by Cre-loxP technology and confirmed the specificity of the model by evaluating (P)RR expression in different tissues as well as adipocyte specific protein expression in all adipose tissues studied. The rate of gene deletion observed are in line with previous studies which have shown that the AP2-Cre^{Salk} mice generated a 50–80% labeling when breeding with a fluorescent reporter gene line [19]. This moderate deletion, however, allows us to make a better link between the phenotypes observed and the effects of the (P)RR gene. Figure 6 summarizes the metabolic alterations induced by adipose tissue (P)RR deletion. Interestingly, both male and female adipose tissue specific (P)RR KO mice had decreased body weights, which were associated with decreased fat masses without any change in food intake. As this phenotype was less pronounced in female mice, given that they are hemizygous KO, total fat mass and adipocyte size were decreased significantly only in male mice. Importantly, this did not result in increased circulating or liver lipid levels but was associated with reduced skeletal muscle TG content but only in male mice. This leaner phenotype could be caused in part by the increased locomotor activity observed in both male and female KO mice during their active period. Furthermore, the more accentuated phenotype observed in males may result from an increase in basal metabolic rate shown by the elevated O₂ consumption and CO₂

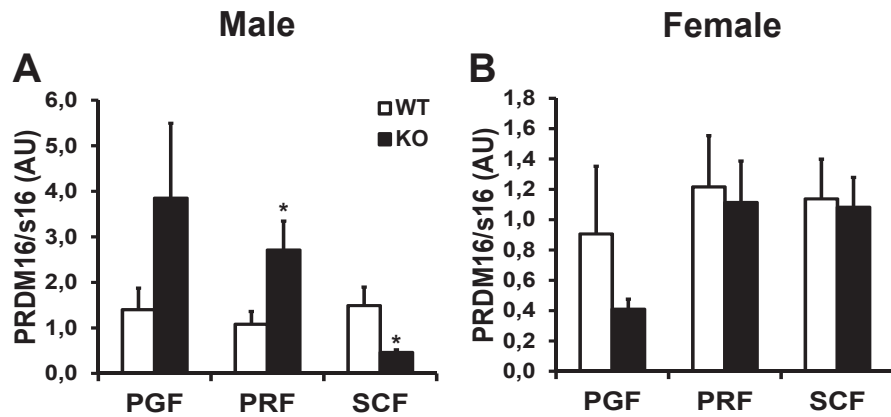


Figure 4: Adipose tissue (P)RRR gene deletion increases a marker of "being" in PRF of male mice. PRDM16 mRNA levels in adipose tissue of male (A) and female (B) mice fed ND. Data are normalized to s16 mRNA levels and are presented as mean \pm SE with $n = 4-10$ per group. * $p < 0.05$ compared to WT. KO, knock-out; PGF, perigonadal fat; PRDM16, PR domain containing 16; PRF, perirenal fat; SCF, abdominal subcutaneous fat; WT, wild-type.

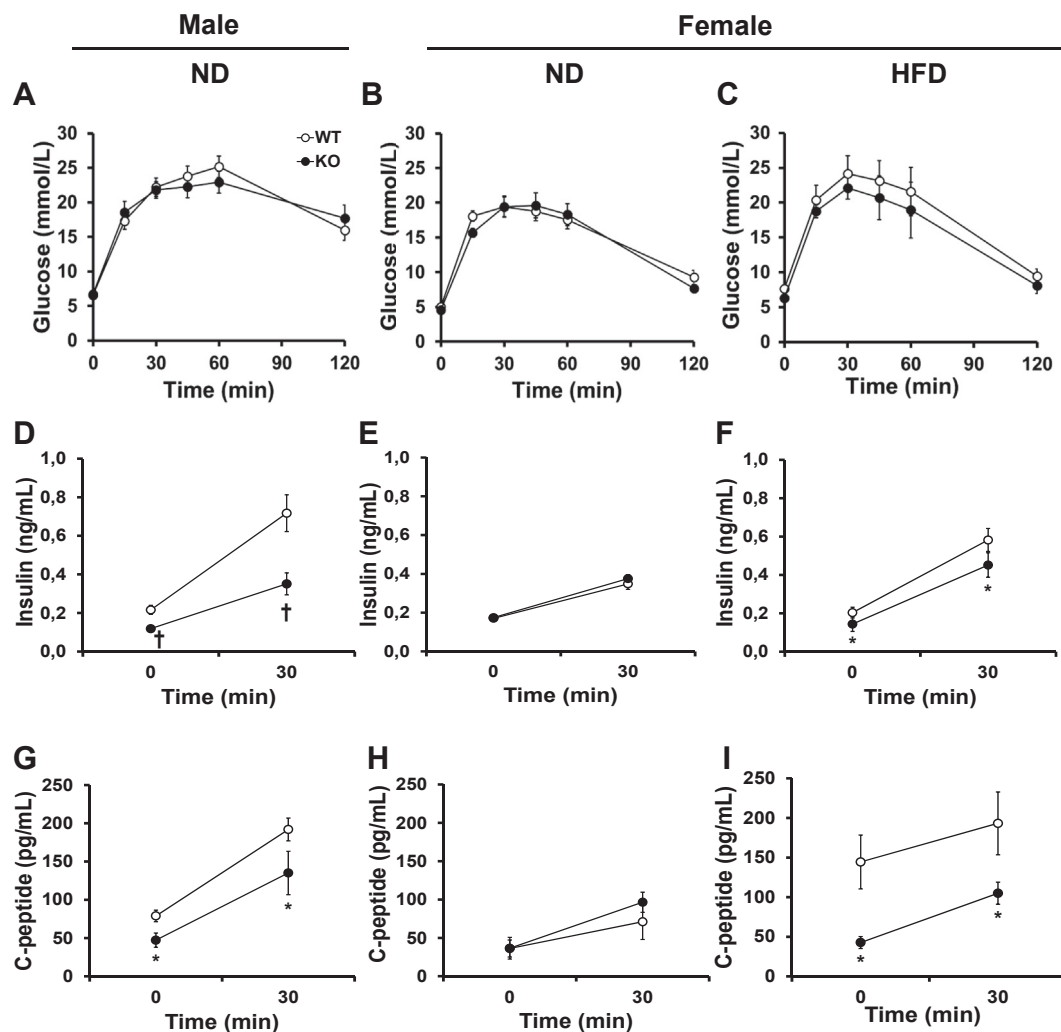


Figure 5: Adipose tissue (P)RRR gene deletion leads to increased insulin sensitivity in male mice. Plasma glucose levels during an OGTT (A, B, C). Basal and stimulated plasma insulin (D, E, F) and C-peptide (G, H, I) levels. Data are presented as mean \pm SE with $n = 9-14$ per group. * $p < 0.05$ and † $p < 0.01$ compared to WT. HFD, high-fat diet; KO, knock-out; ND, normal diet; WT, wild-type.

Table 1 — Effect of adipose tissue (P)RR gene deletion on circulating parameters.

Gender	Male				Female	
	ND		ND		HFD	
Diet	ND		ND		HFD	
Genotype	WT	KO	WT	KO	WT	KO
PRA (ng Ang/mL/h)	25.4 ± 3.0	21 ± 4.1	40.8 ± 6.7	39.0 ± 6.3	40.7 ± 11.4	37.1 ± 10.7
Leptin (ng/mL)	30.35 ± 6.55	10.26 ± 3.07†	10.17 ± 1.77	11.25 ± 2.07	131.89 ± 25.82	121.07 ± 20.61
Adiponectin (pg/mL)	1.98 ± 0.08	2.92 ± 0.13†	1.42 ± 0.05	1.82 ± 0.05†	1.07 ± 0.10	1.46 ± 0.05†
Triglycerides (mg/mL)	7.82 ± 1.71	7.82 ± 1.71	3.74 ± 0.43	2.73 ± 0.37	3.54 ± 0.47	4.62 ± 0.75

Data are presented as mean ± SE with *n* = 8–15 per group. †*p* < 0.01 compared to WT. HFD, high-fat diet; KO, knock-out; ND, normal diet; PRA, plasma renin activity; (P)RR, (pro) renin receptor; WT, wild-type.

production both during their active and inactive period while locomotor activity is unchanged during their inactive period.

It is known well that the (P)RR has both Ang II-dependent (by increasing prorenin and renin catalytic activity and therefore Ang II production) and Ang II-independent effects (by its intracellular signaling and adapter function to the V-ATPase). Of note, a decrease in (P)RR expression leads to a decrease in Ang II production while KOs of other components of the RAS (such as Agt KO) totally abrogate Ang II production. Our observations are in line with adipose tissue and systemic KOs of different components of the RAS and various RAS pharmacological inhibitors studied in rodents which reported decreased body weight and fat masses. In addition, although it has not been evaluated with RAS inhibitors, our data are similar to RAS KOs, which also present with increased physical activity and basal metabolic rate [6]. In line with this literature, overexpression of Agt specifically in adipose tissue produces an increase in weight gain along with a decrease in physical activity [6]. In contrast, adipose tissue-specific Agt KO mouse models do not have any metabolic alterations [39,40] although this may result from the uptake of circulating Agt or Ang II into the adipose tissue, which would compensate for the local deletion. Given that our deletion of the (P)RR gene induces similar but not identical changes in body weight compared to other RAS-KO mouse models (where Ang II production is abrogated), our results strongly suggest that the (P)RR KO effects result from both Ang II-dependent and -independent signaling.

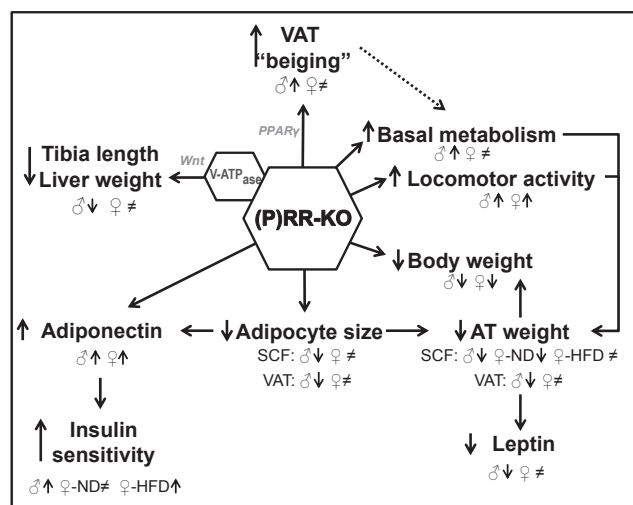


Figure 6: Summary of the metabolic alterations induced by adipose tissue (P)RR gene deletion. Dashed arrows indicate potential mechanism. The ♀ symbol alone is used when the effect is observed in female mice on either ND or HFD. When the effect is different, the signs ♀-ND and ♀-HFD are used.

Adipose tissue-specific modulation of the RAS can directly affect fat mass development. Indeed, it has been shown that Ang II can favor adipogenesis and lipogenesis through the activation of the AT2R and inhibits lipolysis through its binding to the AT1R, therefore promoting lipid accumulation [41]. As such, by decreasing the expression of adipose tissue (P)RR, we may have caused a decrease in renin and prorenin catalytic activity, leading to a reduction in Ang II production, which consequently lowered lipid accumulation, as observed in our model. In addition to the reduction in fat mass, we are the first group, to our knowledge, to show that a reduction in (P)RR expression in adipose tissue can contribute to the browning of white adipose tissue, which is functionally reflected by the increased resting and active metabolic rate of our male KO animals in addition to the elevation in PRDM16 expression in visceral fat pads. Furthermore, the higher lean body mass observed in male KO mice may also contribute to this elevated metabolic rate. Indeed, the 29% higher total lean mass observed in these mice may result from an increased muscle mass due to their elevated locomotor activity, and increased muscle mass is typically associated with an increased metabolic rate [42]. In addition, this increased basal metabolic rate may be caused in part by white adipose being, which is suggested by the observed increase in Prdm16 in our study. These results are in line with previous results obtained by our group in which systemic (P)RR inhibitor administration caused an increase in the expression of ‘being’ markers in white adipose tissue potentially through the activation of PPAR γ (Figure 6) [43]. It also confirms the implication of the RAS in the regulation of thermogenesis initially demonstrated by Takahashi et al. in which whole body renin KO mice demonstrated elevated metabolic rate associated with an increased expression of uncoupling protein 1 in adipose tissues and, as a result, increased thermogenesis [44]. Interestingly, being of white adipose tissue has not been observed in other RAS KO models. As such, the observations in the renin KO mice may result from a link with the (P)RR.

In addition to the smaller fat mass, lack of (P)RR leads to a “healthier” adipose tissue structure. Indeed, larger adipocyte size has been linked with insulin resistance and development of obesity in humans and animal models [45]. Also, increased Ang II has been associated with increased adipocyte size and number, which would contribute to the development of obesity [46–48]. In line with these data, many RAS KO animals have been reported to have smaller adipocytes [44,49,50]. Hence, the smaller adipocyte size observed in our male KO mice may result from reduced Ang II production given the absence of the (P)RR. However, this decreased adipocyte size was not observed in our female KO mice, not even in those fed a HFD. Thus, this may explain why differences in insulin responses and fat pad size are more pronounced in male compared to female KO mice.

In line with the ‘healthier’ adipose tissue structure, our data suggest that (P)RR KO mice (males fed a ND and females fed a HFD) have better

insulin sensitivity than WT mice. Indeed, although we observe no change in the glucose tolerance during an OGTT, circulating insulin concentrations were reduced. The reduced fat mass, increased lean body mass, and plasma adiponectin levels found in the KO mice might have contributed to the increased insulin sensitivity. Interestingly, although we found no modification in many parameters, for instance fat mass and glucose homeostasis, nonetheless, in female mice fed a ND, we observed a modification in circulating adiponectin. This suggests that the change may be an initiating factor in the modulation of glucose homeostasis by (P)RR that precedes the significant changes in fat pad mass. Furthermore, this is in line with our recent publication which reported that systemic HRP administration to HFD fed mice can improve circulating adiponectin concentration. This is also in agreement with previous publications showing that Ang II decreases adiponectin gene expression and plasma levels, whereas RAS inhibitors increase plasma adiponectin levels [51,52]. However, in other RAS suppression models, both glucose and insulin levels were decreased to produce an improved glucose homeostasis [42,44,49,50,53]. More recently, Wu et al. reported that adipose tissue (P)RR KO mice have no change in glucose tolerance when fed a ND but show increased plasma insulin levels [54]. This change in insulin levels, which is different from our observations, could be attributed in part to the severe lipodystrophy and liver steatosis present in their model, leading to a decrease in insulin clearance [54,55]. Indeed, by using the adiponectin-Cre, known for its high efficiency in gene deletion and robust adipose-tissue specificity [19], Wu et al. demonstrate the effect of a more severe (80% decrease) (P)RR deletion while our model shows a dose-dependent effect (as differences in phenotypes can be observed between the hemizygous KO females and the homozygous KO males) induced by a milder (between 30 and 50%, respectively) decrease in (P)RR gene expression as we used the AP2-Cre mouse. These levels of deletion are in line with a previous study, which demonstrated that the AP2-Cre^{Salk} mice generated a 50–80% labeling when breeding with a fluorescent reporter gene line while the Adiponectin-Cre generated a near 100% recombination [19].

In line with the developmental defects associated with (P)RR KOs described in the literature [14,15], we found that adipose-tissue specific (P)RR deletion led to a 50% reduction in the expected number of KO male pups born. Given that this effect has not been reported in adipose-specific RAS KO models, we propose that Ang II-independent effects mediated by the (P)RR may play a role in fetal development, due to its association with V-ATPase and its concomitant regulation of the Wnt-signaling cascade. Moreover, in addition to their lower adiposity, we have shown that male KO mice are markedly shorter and have reduced liver weight, despite a similar food intake, compared to WT male mice. We did not observe such differences in hemizygous female (P)RR KO mice possibly because the gene deficiency is only partial.

Interestingly, the data presented here are very much in line with those previously published by our group which have shown that the administration of HRP, a (P)RR blocker, to mice fed a HFD also reduces body weight gain through decreased fat mass and seems to improve insulin sensitivity by improving adiponectin profile [18]. Taken together, our results suggest that adipose tissue (P)RR is involved in the development of obesity and its associated complications. Indeed, suppression of the (P)RR specifically in adipose tissue produced a clear phenotype of reduced body weight and fat masses as well as improved adipose tissue structure and insulin sensitivity. This indicates that adipose tissue (P)RR may be an important target for the development of new drugs for the treatment of obesity and type 2 diabetes. For instance, a more effective approach for the treatment of diabetes and its complications could be to combine the classical RAS inhibitors with

a (P)RR blocker such as the HRP. This would block the Ang II-independent pathways, further reduce Ang II-dependent pathways, and prevent associated end-organ damage. However, in line with the study from Wu et al., it would be of the upmost importance to carefully monitor the downregulation of the (P)RR activity to prevent lipodystrophy and the concomitant liver steatosis.

FUNDING

This study was supported by a Canadian Diabetes Association and Heart and Stroke Foundation of Canada operating Grant. OS is supported by MSMT LK112.

ACKNOWLEDGEMENTS

We thank the Cell Physiology and Rodent Cardiovascular Phenotyping core facility of the CRCHUM for the measurement of plasma insulin, C-peptide, adiponectin and leptin and access to the Echo-MRI. We thank Catherine Michel, Sonia Kajla, and Zhenhong Li for their technical assistance. This work was supported by a Canadian Diabetes Association and Heart and Stroke Foundation of Canada operating Grant. OS is supported by MSMT LK11217.

CONFLICT OF INTEREST

None declared.

APPENDIX A. SUPPLEMENTARY DATA

Supplementary data related to this article can be found at <http://dx.doi.org/10.1016/j.molmet.2016.08.009>.

REFERENCES

- [1] James, W.P., 2008. WHO recognition of the global obesity epidemic. *International Journal of Obesity (London)* 32(Suppl 7):S120–S126. <http://dx.doi.org/10.1038/ijo.2008.247> [pii].
- [2] Shaw, J.E., Sicree, R.A., Zimmet, P.Z., 2010. Global estimates of the prevalence of diabetes for 2010 and 2030. *Diabetes Res Clin Pract* 87(4–14). <http://dx.doi.org/10.1016/j.diabres.2009.10.007>. S0168–8227(09)00432-X [pii].
- [3] Yiannikouris, F., Gupte, M., Putnam, K., Thatcher, S., Charnigo, R., Rateri, D.L., et al., 2012. Adipocyte deficiency of angiotensinogen prevents obesity-induced hypertension in male mice. *Hypertension* 60:1524–1530. <http://dx.doi.org/10.1161/HYPERTENSIONAHA.112.192690>. HYPERTENSIONAHA.112.192690 [pii].
- [4] Sarzani, R., Salvi, F., Dessi-Fulgheri, P., Rappelli, A., 2008. Renin-angiotensin system, natriuretic peptides, obesity, metabolic syndrome, and hypertension: an integrated view in humans. *Journal of Hypertension* 26:831–843. <http://dx.doi.org/10.1097/HJH.0b013e3282f624a0>, 00004872-200805000-00001 [pii].
- [5] Frigolet, M.E., Torres, N., Tovar, A.R., 2013. The renin-angiotensin system in adipose tissue and its metabolic consequences during obesity. *Journal of Nutritional Biochemistry* 24:2003–2015.
- [6] Littlejohn, N.K., Grobe, J.L., 2015. Opposing tissue-specific roles of angiotensin in the pathogenesis of obesity, and implications for obesity-related hypertension. *American Journal of Physiology Regulatory Integrative and Comparative Physiol* 309:R1463–R1473. <http://dx.doi.org/10.1152/ajpregu.00224.2015> [pii].
- [7] Nguyen, G., Delarue, F., Burckle, C., Bouzahir, L., Gillier, T., Sraer, J.D., 2002. Pivotal role of the renin/prorenin receptor in angiotensin II production and cellular responses to renin. *Journal of Clinical Investigation* 109:1417–1427.
- [8] Montani, J.P., Van Vliet, B.N., 2004. General Physiology and pathophysiology of the renin-angiotensin system. *Handb Exp Pharmacol* 1:3–29.

- [9] Fletcher, S.J., Kalupahana, N.S., Soltani-Bejnood, M., Kim, J.H., Saxton, A.M., Wasserman, D.H., et al., 2012. Transgenic mice overexpressing Renin exhibit glucose intolerance and diet-genotype interactions. *Frontiers in Endocrinology (Lausanne)* 3(166). <http://dx.doi.org/10.3389/fendo.2012.00166>.
- [10] Kalupahana, N.S., Moustaid-Moussa, N., 2012. The renin-angiotensin system: a link between obesity, inflammation and insulin resistance. *Obesity Reviews* 13:136–149. <http://dx.doi.org/10.1111/j.1467-789X.2011.00942.x>.
- [11] Ahmed, B.A., Seda, O., Lavoie, J.L., 2011. (Pro)renin receptor as a new drug target. *Current Pharmaceutical Design* 17:3611–3621. BSP/CPD/E-Pub/000738 [pii].
- [12] Danser, A.H., van Kesteren, C.A., Bax, W.A., Tavenier, M., Derckx, F.H., Saxena, P.R., et al., 1997. Prorenin, renin, angiotensinogen, and angiotensin-converting enzyme in normal and failing human hearts. Evidence for renin binding. *Circulation* 96:220–226.
- [13] Brown, M.J., 2007. Renin: friend or foe? *Heart* 93:1026–1033 <http://dx.doi.org/10.1136/hrt.2006.107706> hrt.2006.107706 [pii].
- [14] Amsterdam, A., Nissen, R.M., Sun, Z., Swindell, E.C., Farrington, S., Hopkins, N., 2004. Identification of 315 genes essential for early zebrafish development. *Proc Natl Acad Sci U S A* 101:12792–12797. <http://dx.doi.org/10.1073/pnas.0403929101>, 0403929101 [pii].
- [15] Cruciati, C.M., Ohkawara, B., Acebron, S.P., Karaulanov, E., Reinhard, C., Ingelfinger, D., et al., 2010. Requirement of prorenin receptor and vacuolar H⁺-ATPase-mediated acidification for Wnt signaling. *Science* 327:459–463. <http://dx.doi.org/10.1126/science.1179802>, 327/5964/459 [pii].
- [16] Kinouchi, K., Ichihara, A., Sano, M., Sun-Wada, G.H., Wada, Y., Kurauchi-Mito, A., et al., 2010. The (pro)renin receptor/ATP6AP2 is essential for vacuolar H⁺-ATPase assembly in murine cardiomyocytes. *Circulation Research* 107:30–34. <http://dx.doi.org/10.1161/CIRCRESAHA.110.224667>. CIRCRESAHA.110.224667 [pii].
- [17] Oshima, Y., Kinouchi, K., Ichihara, A., Sakoda, M., Kurauchi-Mito, A., Bokuda, K., et al., 2011. Prorenin receptor is essential for normal podocyte structure and function. *Journal of the American Society of Nephrology* 22:2203–2212. <http://dx.doi.org/10.1681/ASN.2011020202>. ASN.2011020202 [pii].
- [18] Tan, P., Shamansurova, Z., Bisotto, S., Michel, C., Gauthier, M.S., Rabasa-Lhoret, R., et al., 2014. Impact of the prorenin/renin receptor on the development of obesity and associated cardiometabolic risk factors. *Obesity (Silver Spring)* 22:2201–2209. <http://dx.doi.org/10.1002/oby.20844>.
- [19] Jeffery, E., Berry, R., Church, C.D., Yu, S., Shook, B.A., Horsley, V., et al., 2014. Characterization of Cre recombinase models for the study of adipose tissue. *Adipocyte* 3:206–211. <http://dx.doi.org/10.4161/adip.29674>, 2014ADIPOCYTE206R [pii].
- [20] Lee, K.Y., Russell, S.J., Ussar, S., Boucher, J., Vernochet, C., Mori, M.A., et al., 2013. Lessons on conditional gene targeting in mouse adipose tissue. *Diabetes* 62:864–874. <http://dx.doi.org/10.2337/db12-1089> db12-1089 [pii].
- [21] Truett, G.E., Heeger, P., Mynatt, R.L., Truett, A.A., Walker, J.A., Warman, M.L., 2000. Preparation of PCR-quality mouse genomic DNA with hot sodium hydroxide and tris (HotSHOT). *Biotechniques* 29, 52–+.
- [22] Truett, G.E., Heeger, P., Mynatt, R.L., Truett, A.A., Walker, J.A., Warman, M.L., 2000. High-throughput preparation of PCR-quality mouse genomic DNA with hot sodium hydroxide and tris (HotSHOT). *FASEB Journal* 14:A53.
- [23] Genest, D.S., Falcao, S., Michel, C., Kajla, S., Germano, M.F., Lacasse, A.A., et al., 2013. Novel role of the renin-angiotensin system in preeclampsia superimposed on chronic hypertension and the effects of exercise in a mouse model. *Hypertension* 62:1055–1061. <http://dx.doi.org/10.1161/HYPERTENSIONAHA.113.01983>. HYPERTENSIONAHA.113.01983 [pii].
- [24] de Kloet, A.D., Krause, E.G., Scott, K.A., Foster, M.T., Herman, J.P., Sakai, R.R., et al., 2011. Central angiotensin II has catabolic action at white and brown adipose tissue. *American Journal of Physiology Endocrinology and Metabolism* 301:E1081–E1091. <http://dx.doi.org/10.1152/ajpendo.00307.2011> ajpendo.00307.2011 [pii].
- [25] Ferrannini, E., 1988. The theoretical bases of indirect calorimetry — a review. *Metabolism—Clinical and Experimental* 37:287–301.
- [26] Lambert, M.I., Noakes, T.D., 1990. Spontaneous running increases V_{O2}max and running performance in rats. *Journal of Applied Physiology* 68:400–403.
- [27] Tura, A., Kautzky-Willer, A., Pacini, G., 2006. Insulinogenic indices from insulin and C-peptide: comparison of beta-cell function from OGTT and IVGTT. *Diabetes Research and Clinical Practice* 72(298–301). <http://dx.doi.org/10.1016/j.diabres.2005.10.005>. S0168–8227(05)00408-0 [pii].
- [28] Andrikopoulos, S., Blair, A.R., Deluca, N., Fam, B.C., Proietto, J., 2008. Evaluating the glucose tolerance test in mice. *American Journal of Physiology-Endocrinology and Metabolism* 295:E1323–E1332.
- [29] Szeto, I.M.Y., Das, P.J., Taha, A.Y., Aziz, A., Anderson, G.H., 2005. Effect of increased multivitamin intake of rats during pregnancy on food intake and glucose metabolism of male offspring. *FASEB Journal* 19:A1702.
- [30] Efferchichi, M., Mercier, J., Coisy-Quivy, M., Metz, L., Lajoix, A.D., Gross, R., et al., 2010. Effects of exposure to a 128-mT static magnetic field on glucose and lipid metabolism in serum and skeletal muscle of rats. *Archives of Medical Research* 41(309–314). <http://dx.doi.org/10.1016/j.arcmed.2010.07.008>. S0188–4409(10)00191-8 [pii].
- [31] Singh, P., Deng, A., Weir, M.R., Blantz, R.C., 2008. The balance of angiotensin II and nitric oxide in kidney diseases. *Current Opinion in Nephrology and Hypertension* 17:51–56. <http://dx.doi.org/10.1097/MNH.0b013e3282f29a8b>, 00041552-200801000-00009 [pii].
- [32] Valorani, M.G., Hawa, M.I., Buckley, L.R., Afeltra, A., Cacciapaglia, F., Pozzilli, P., 2004. The natural history of insulin content in the pancreas of female and male non-obese diabetic mouse: implications for trials of diabetes prevention in humans. *Diabetes-Metabolism Research and Reviews* 20:394–398.
- [33] Hausman, D.B., Park, H.J., Hausman, G.J., 2008. Isolation and culture of pre-adipocytes from rodent white adipose tissue. *Methods in Molecular Biology* 456:201–219. http://dx.doi.org/10.1007/978-1-59745-245-8_15.
- [34] Schneider, C.A., Rasband, W.S., Eliceiri, K.W., 2012. NIH Image to ImageJ: 25 years of image analysis. *Nature Methods* 9:671–675.
- [35] Cypess, A.M., Lehman, S., Williams, G., Tal, I., Rodman, D., Goldfine, A.B., et al., 2009. Identification and importance of brown adipose tissue in adult humans. *New England Journal of Medicine* 360:1509–1517.
- [36] van Engelen, M.A., Nielsen, M.K., Ribeiro, E.L., 1995. Differences in pup birth weight, pup variability within litters, and dam weight of mice selected for alternative criteria to increase litter size. *Journal of Animal Science* 73:1948–1953.
- [37] Harms, M., Seale, P., 2013. Brown and beige fat: development, function and therapeutic potential. *Nature Medicine* 19:1252–1263. <http://dx.doi.org/10.1038/nm.3361> nm.3361 [pii].
- [38] Frayn, K.N., Arner, P., Yki-Jarvinen, H., 2006. Fatty acid metabolism in adipose tissue, muscle and liver in health and disease. *Essays in Biochemistry* 42:89–103. <http://dx.doi.org/10.1042/bse0420089> bse0420089 [pii].
- [39] Yiannikouris, F., Karounos, M., Charnigo, R., English, V.L., Rateri, D.L., Daugherty, A., et al., 2012. Adipocyte-specific deficiency of angiotensinogen decreases plasma angiotensinogen concentration and systolic blood pressure in mice. *American Journal of Physiology-Regulatory Integrative and Comparative Physiology* 302:R244–R251.
- [40] LeMieux, M.J., Ramalingam, L., Mynatt, R.L., Kalupahana, N.S., Kim, J.H., Moustaid-Moussa, N., 2016. Inactivation of adipose angiotensinogen reduces adipose tissue macrophages and increases metabolic activity. *Obesity (Silver Spring)* 24:359–367. <http://dx.doi.org/10.1002/oby.21352>.
- [41] Yvan-Charvet, L., Quignard-Boulange, A., 2011. Role of adipose tissue renin-angiotensin system in metabolic and inflammatory diseases associated with obesity. *Kidney International* 79:162–168. <http://dx.doi.org/10.1038/ki.2010.391> ki2010391 [pii].
- [42] Jayasooriya, A.P., Mathai, M.L., Walker, L.L., Begg, D.P., Denton, D.A., Cameron-Smith, D., et al., 2008. Mice lacking angiotensin-converting enzyme have increased energy expenditure, with reduced fat mass and improved

- glucose clearance. *Proceedings of the National Academy of Sciences U S A* 105: 6531–6536. <http://dx.doi.org/10.1073/pnas.0802690105>, 0802690105 [pii].
- [43] Tan, P., Blais, C., Nguyen, T.M., Schiller, P.W., Gutkowska, J., Lavoie, J.L., 2016. Prorenin/renin receptor blockade promotes a healthy fat distribution in obese mice. *Silver Spring: Obesity*. <http://dx.doi.org/10.1002/oby.21592>.
- [44] Takahashi, N., Li, F., Hua, K., Deng, J., Wang, C.H., Bowers, R.R., et al., 2007. Increased energy expenditure, dietary fat wasting, and resistance to diet-induced obesity in mice lacking renin. *Cell Metabolism* 6(506–512). <http://dx.doi.org/10.1016/j.cmet.2007.10.011>. S1550–4131(07)00304-X [pii].
- [45] Guilherme, A., Virbasius, J.V., Puri, V., Czech, M.P., 2008. Adipocyte dysfunctions linking obesity to insulin resistance and type 2 diabetes. *Nature Reviews Molecular Cell Biology* 9:367–377. <http://dx.doi.org/10.1038/nrm2391> nrm2391 [pii].
- [46] Crandall, D.L., Armellino, D.C., Busler, D.E., McHendry-Rinde, B., Kral, J.G., 1999. Angiotensin II receptors in human preadipocytes: role in cell cycle regulation. *Endocrinology* 140:154–158.
- [47] Darimont, C., Vassaux, G., Ailhaud, G., Negrel, R., 1994. Differentiation of preadipose cells: paracrine role of prostacyclin upon stimulation of adipose cells by angiotensin-II. *Endocrinology* 135:2030–2036.
- [48] Lyle, R.E., Habener, J.F., McGehee Jr., R.E., 1996. Antisense oligonucleotides to differentiation-specific element binding protein (DSEB) mRNA inhibit adipocyte differentiation. *Biochem Biophys Res Commun* 228:709–715. S0006291X96917210 [pii].
- [49] Massiera, F., Bloch-Faure, M., Ceiler, D., Murakami, K., Fukamizu, A., Gasc, J.M., et al., 2001. Adipose angiotensinogen is involved in adipose tissue growth and blood pressure regulation. *FASEB Journal* 15:2727–2729.
- [50] Massiera, F., Seydoux, J., Geloën, A., Quignard-Boulange, A., Turban, S., Saint-Marc, P., et al., 2001. Angiotensinogen-deficient mice exhibit impairment of diet-induced weight gain with alteration in adipose tissue development and increased locomotor activity. *Endocrinology* 142:5220–5225.
- [51] Furuhashi, M., Ura, N., Higashiura, K., Murakami, H., Tanaka, M., Moniwa, N., et al., 2003. Blockade of the renin-angiotensin system increases adiponectin concentrations in patients with essential hypertension. *Hypertension* 42:76–81. <http://dx.doi.org/10.1161/01.HYP.0000078490.59735.6E>, 01.HYP.0000078490.59735.6E [pii].
- [52] Frantz, E.D., Crespo-Mascarenhas, C., Barreto-Vianna, A.R., Aguilá, M.B., Mandarin-de-Lacerda, C.A., 2013. Renin-angiotensin system blockers protect pancreatic islets against diet-induced obesity and insulin resistance in mice. *PLoS One* 8:e67192. <http://dx.doi.org/10.1371/journal.pone.0067192>. PONE-D-13-07860 [pii].
- [53] Ishida, J., Sugiyama, F., Tanimoto, K., Taniguchi, K., Syouji, M., Takimoto, E., et al., 1998. Rescue of angiotensinogen-knockout mice. *Biochemical and Biophysical Research Communications* 252:610–616.
- [54] Wu, C.H., Mohammadmoradi, S., Thompson, J., Su, W., Gong, M., Nguyen, G., et al., 2016. Adipocyte (Pro)Renin-Receptor deficiency induces lipodystrophy, liver steatosis and increases blood pressure in male mice. *Hypertension* 68: 213–219. <http://dx.doi.org/10.1161/HYPERTENSIONAHA.115.06954>. HYPERTENSIONAHA.115.06954 [pii].
- [55] Bril, F., Lomonaco, R., Orsak, B., Ortiz-Lopez, C., Webb, A., Tio, F., et al., 2014. Relationship between disease severity, hyperinsulinemia, and impaired insulin clearance in patients with nonalcoholic steatohepatitis. *Hepatology* 59: 2178–2187, 10.1002/hep.26988 [doi].

Supplementary Table 1. Primer sequences for PCR and qPCR

Primers	Oligonucleotide sequences	PCR conditions and cycles
(P)RR-LoxP	5'-CTGGATCCCGGAGCATGGGTAAAGG-3'	H: 95 °C, 5 min; D: 95 °C, 30 sec;
	5'-CAGGTGTGCTGCTATTAATAGG-3'	A: 60 °C, 30 sec; E: 72°C, 45 sec;
	5'-GCCCCTCTCTTACAGTTCTATCAGT-3'	Cycles : 40
	5'-AGCACTCTCTTCCAGGTATGTTGTG-3'	
Cre-recombinase	5'-CTAGGCCACAGAATTGAAAGATCT-3'	H: 95 °C, 5 min; D: 95 °C, 30 sec;
	5'-GTAGGTGGAAATTCTAGCATCATCC-3'	A: 60 °C, 30 sec; E: 72 °C, 45 sec;
	5'-GCGGTCTGGCAGTAAAACTATC-3'	Cycles : 40
X/Y chromosome	5'-GTGAAACAGCATTGCTGTCACTT-3'	
	5'-GAAGTGAATTGAAGTTTTGGTCTAG-3'	H: 95 °C, 5 min; D: 95 °C, 30 sec;
	5'-GGGACCTAACTGTTGGCTTTATCAG-3'	A: 60 °C, 30 sec; E: 72 °C, 45 sec;
	5'-CCTATGAAATCCTTTGCTGCACATGT-3'	Cycles : 40
	5'-AAGATAAGCTTACATAATCACATGGA-3'	
(P)RR	F - 5'-TTTGGATGAACTTGGGAAGC-3'	H: 95 °C, 15 min; D: 95 °C 15 sec;
	R - 3'-CACAAGGGATGTGTCTGAATG-5'	A: 60 °C 30 sec; E: 72 °C 30 sec;
18s		Cycles : 40
	F - 5'-CTGAGAAACGGCTACCACATC-3'	H: 95 °C 15 min; D: 95 °C 15 sec;
	R - 3'-GGCCTCGAAAGAGTCCTGTAT-5'	A: 60 °C 30 sec; E: 72 °C 30 sec;
		Cycles : 40
s16	F - 5'-ATCTCAAAGGCCCTGGTAGC-3'	H: 95 °C, 10 min; D: 95 °C 15 sec;
	R - 5'ACAAAGGTAAACCCCGATCG-3'	A: 60 °C 30 sec; E: 72 °C 30 sec;
		Cycles : 40

PRDM16 F - 5'-GCCATGTGTCAGATCAACGA-3' H: 95 °C, 10 min; D: 95 °C 15 sec;
A: 60 °C 30 sec; E: 72 °C 30 sec;
R - 5'-CCTTCTTTCACATGCACCAA-3' Cycles : 40

A, annealing; AP2, adipocyte protein 2; D, denaturation; E, elongation; F, forward; H, hold; (P)RR,
(pro)renin receptor; R, reverse.

Supplementary Table 2. Foetal weight in AP2Cre/(P)RRLoxP strain

Genotype	Male weight (g)	Female weight (g)
(male/female ratio)		
WT (4/5)	0.90 ± 0.02	0.84 ± 0.03*
KO (7/7)	0.90 ± 0.03	0.88 ± 0.04*
Lox-p (6/9)	0.88 ± 0.03	0.87 ± 0.04
Cre (1/8)	0.93 ± 0.10	0.88 ± 0.02*

Data are presented as mean ± SE. * $p < 0.05$ compared to male pups. n per group is indicated in parenthesis. AP2, adipocyte protein 2; KO, knock-out; (P)RR, (pro)renin receptor; WT, wild-type.

Supplementary Table 3. Average daily calorie intake

Gender	Diet	Genotype	<i>n</i>	kcal/day
Male	ND	WT	14	14.08 ± 0.56
		KO	9	13.35 ± 0.33
Female	ND	WT	24	12.99 ± 0.57
		KO	18	12.21 ± 0.36
	HFD	WT	17	14.01 ± 0.46
		KO	16	13.16 ± 0.48

Data are presented as mean ± SE. HFD, high-fat diet; KO, knock-out; ND, normal diet; WT, wild-type.

Supplementary Table 4. Adipose tissue (P)RR gene deletion effect on adipocyte size in female mice.

Diet	ND		HFD	
Genotype	WT	KO	WT	KO
<i>n</i>	4	5	5	5
SCF (pm²)	3.1 ± 0.9	3.5 ± 0.7	4.4 ± 0.3	4.9 ± 0.4
PGF (pm²)	2.1 ± 0.1	2.8 ± 0.1	4.8 ± 0.4	4.5 ± 0.3
PRF (pm²)	3.4 ± 1.0	3.4 ± 0.9	5.1 ± 0.5	4.4 ± 0.5

Data are presented as mean ± SE. HFD, high-fat diet; KO, knock-out; ND, normal diet; PGF, perigonadal fat; PRF, perirenal fat; (P)RR, (pro)renin receptor; SCF, abdominal subcutaneous fat; WT, wild-type.

Supplementary Table 5. Effect of adipose tissue (P)RR gene deletion on tissue weight and tibia length

Gender	Male		Female			
	ND		ND		HFD	
	WT	KO	WT	KO	WT	KO
Liver/tibia (mg/mm)	87.1 ± 2.4	75.5 ± 3.7*	68.9 ± 2.9	65.5 ± 0.4	61.2 ± 2.5	61.3 ± 2.8
Heart/tibia (mg/mm)	8.8 ± 0.3	8.8 ± 0.4	7.9 ± 0.3	7.3 ± 0.2	8.2 ± 0.4	7.1 ± 0.7
Tibia length (mm)	17.9 ± 0.1	17.3 ± 0.1†	18.0 ± 0.1	17.7 ± 0.2	17.5 ± 0.2	17.4 ± 0.1

Data are presented as mean ± SE with *n* = 7-14 per group. * *p* < 0.05 and † *p* < 0.01 compared to WT.

HFD, high-fat diet; KO, knock-out; ND, normal diet; (P)RR, (pro)renin receptor; WT, wild-type.

Supplementary Table 6. Vertical distance is not modified by adipose tissue (P)RR gene deletion.

Gender	Genotype	Day	Night
	(n)	(cm)	(cm)
Male	WT (7)	482.7 ± 72.5	4748 ± 857.4
	KO (7)	310.3 ± 48.7	5111 ± 426
Female	WT (19)	1598.9 ± 598.6	10292.8 ± 2062.5
	KO (16)	1826.7 ± 503.5	12582.7 ± 2190.4

Data are presented as mean ± SE. HFD, high-fat diet; KO, knock-out; ND, normal diet; (P)RR, (pro)renin receptor; WT, wild-type.

Supplementary Table 7. Effect of adipose tissue (P)RR gene deletion on glucose homeostasis during an OGTT

	Male				Female	
	ND		ND		HFD	
	WT	KO	WT	KO	WT	KO
C-peptide/Insulin (T0)	0.41 ± 0.06	0.52 ± 0.13	0.36 ± 0.08	0.30 ± 0.07	0.76 ± 0.23	0.56 ± 0.17
C-peptide/Insulin (T30)	0.29 ± 0.02	0.40 ± 0.06	0.30 ± 0.10	0.29 ± 0.05	0.39 ± 0.10	0.28 ± 0.04

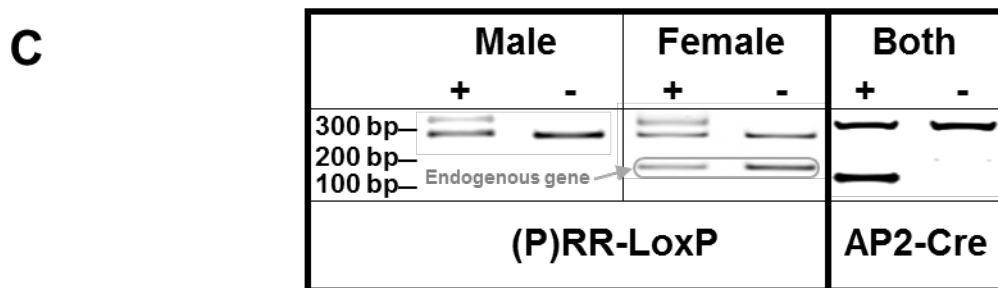
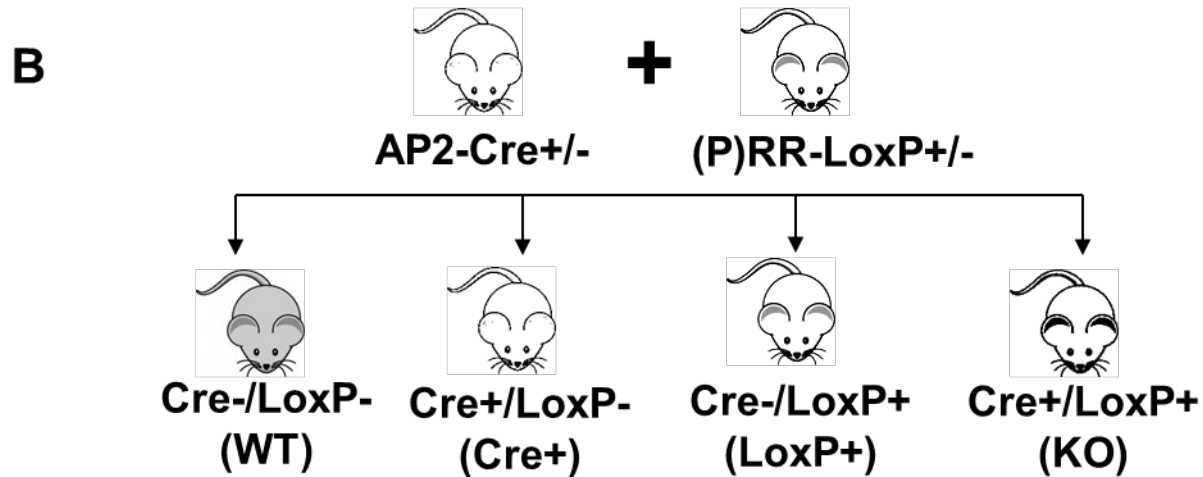
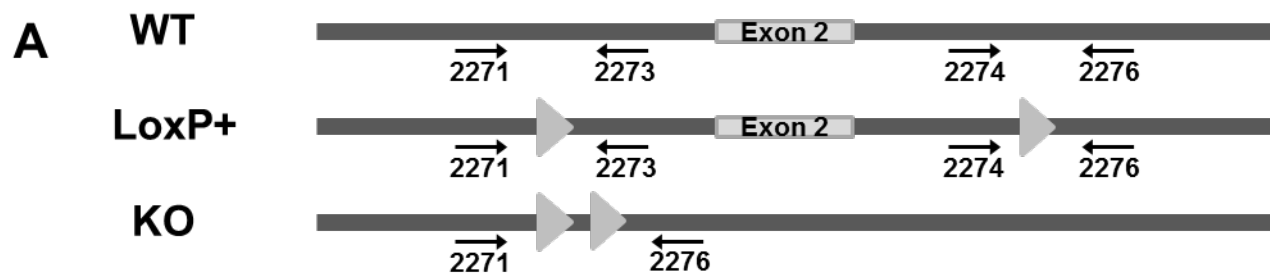
Data are expressed as mean ± SE with $n = 5-19$ per group. KO, knock-out; (P)RR, (pro)renin receptor;

WT, wild-type.

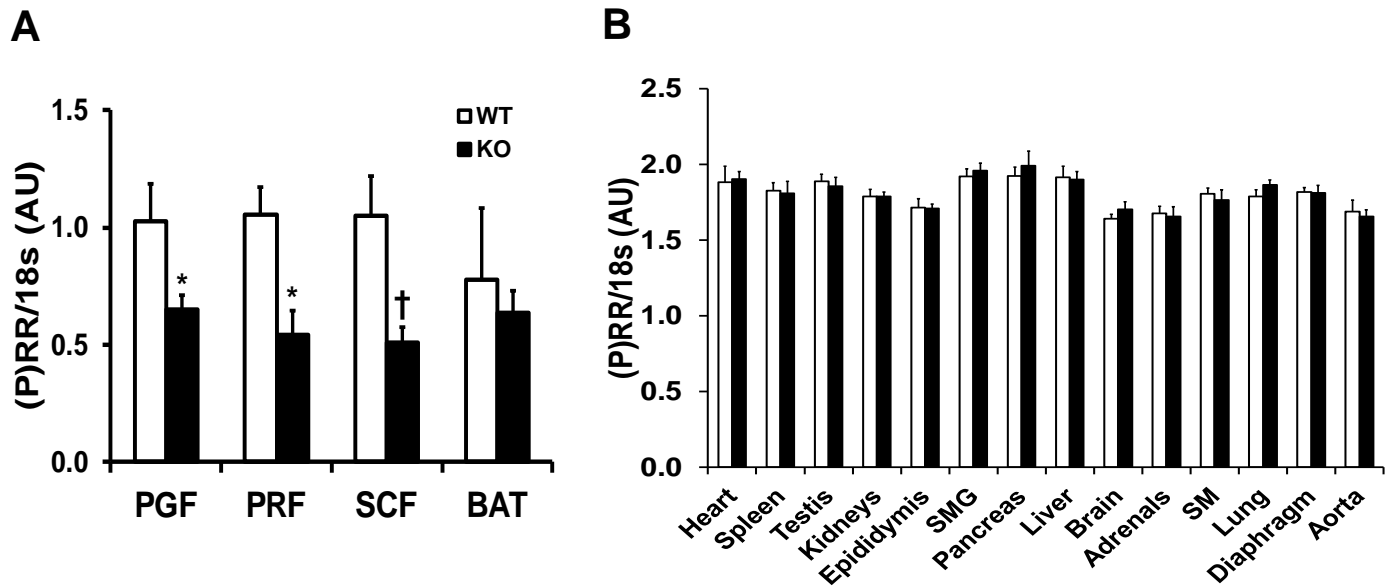
Supplementary Table 8. Effect of adipose tissue (P)RR gene deletion on tissue metabolites

Gender	Male				Female	
Diet	ND		ND		HFD	
Genotype	WT	KO	WT	KO	WT	KO
Total liver triglycerides (mg)	24.6 ± 6.4	18.7 ± 3.5	13.5 ± 2.1	22.9 ± 4.5	73.8 ± 13.5	61.1 ± 11.6
Total muscle triglycerides (µg)	317.0 ± 52.2	83.0 ± 27.1*	177.2 ± 39.5	120.8 ± 31.1	141.1 ± 41.9	163.2 ± 32.0
Total muscle glycerol (µg)	31.5 ± 2.3	22.9 ± 2.6*	27.2 ± 2.5	20.7 ± 2.1	25.3 ± 3.5	27.9 ± 2.9
Total pancreas insulin (µg)	19.4 ± 1.8	23.3 ± 1.5	26.1 ± 1.4	25.1 ± 2.1	25.8 ± 1.4	25.3 ± 1.5

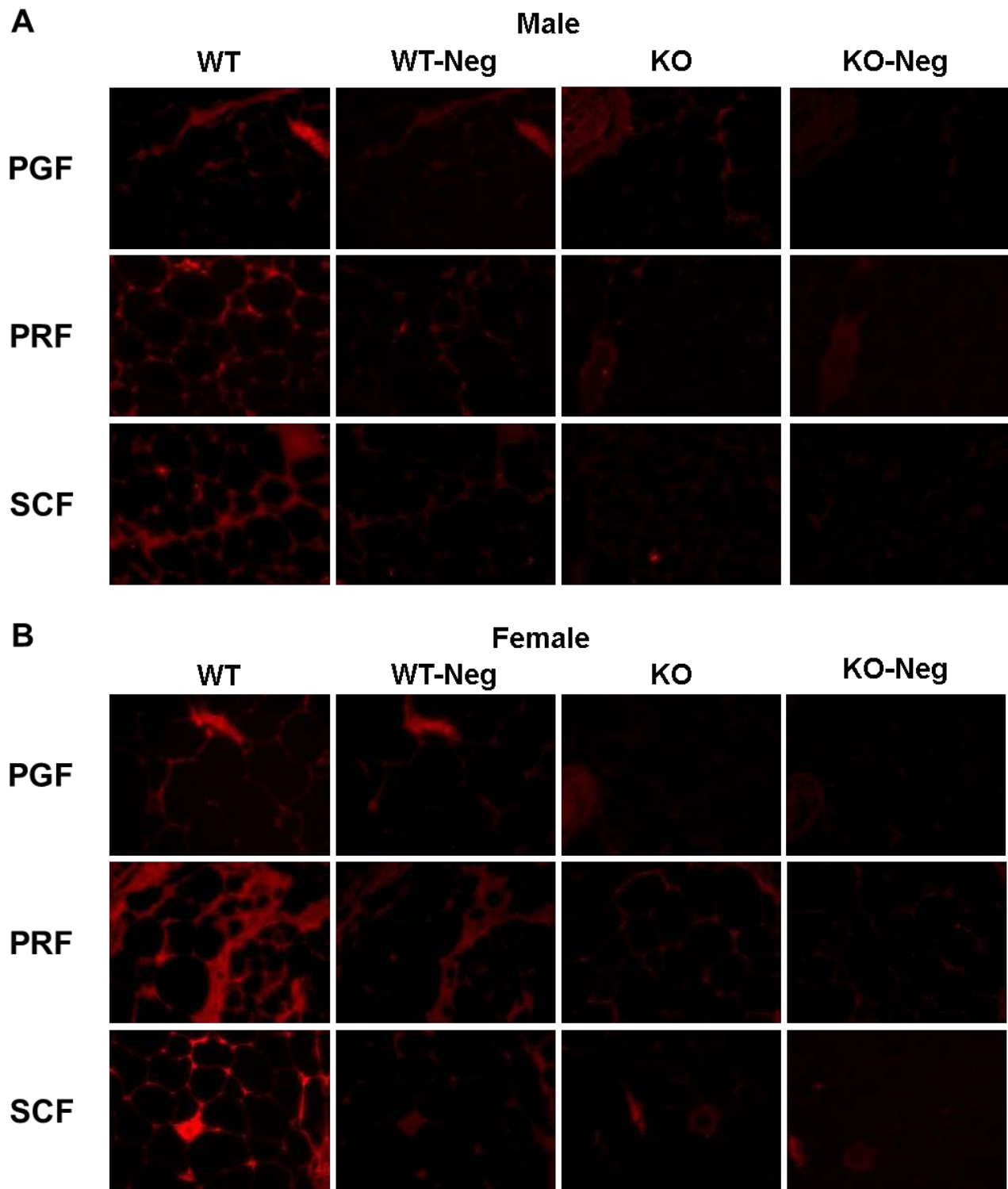
Data are presented as mean ± SE. *n* = 6-14 per group. * *p* < 0.05 compared to WT. HFD, high-fat diet; KO, knock-out; ND, normal diet; (P)RR, (pro)renin receptor; WT, wild-type.



Supplementary Figure 1. Adipose tissue specific (P)RR gene deletion. (A) Adipose tissue specific AP2-Cre/(P)RR-LoxP gene inactivation map. (B) Knock-out (KO) mice were obtained by breeding AP2-Cre+/- with (P)RR-LoxP+/- heterozygous mice. From this breeding, we obtained Cre-/LoxP-/- (WT), Cre+/-LoxP-/- (Cre+), Cre-/LoxP+/- (LoxP+) and Cre+/-LoxP+/- (KO) mice. Because the (pro)renin receptor [(P)RR] gene is located on the X chromosome, male KO mice were homozygous and females were heterozygous. (C) Agarose gel showing genotyping bands patterns for Cre and LoxP.



Supplemental Figure 2. (P)RR gene deletion is specific to adipose tissue. (P)RR mRNA levels in adipose tissues (A) and other tissues (B) in male mice. Data are normalized to 18s mRNA levels and are presented as mean \pm SE with $n = 5-6$ per group. * $p < 0.05$ and † $p < 0.01$ compared to WT. BAT, brown adipose tissue; KO, knock-out; PGF, perigonadal fat; PRF, perirenal fat; (P)RR, (pro)renin receptor; SCF, abdominal subcutaneous fat; SMG, submandibular gland; SM, skeletal muscle; WT, wild-type.



Supplementary Figure 3. (P)RR immunohistochemistry in adipose tissue in male (A) and female (B) mice. KO mice showed a significant decrease in (P)RR staining on adipocyte membranes both in male and female mice. KO, knock-out; PGF, peri-gonadal fat; PRF, peri-renal fat; (P)RR, (pro)renin receptor; SCF, abdominal subcutaneous fat; WT, wild-type.